Comparison of clinical and environmental isolates of *Acanthamoeba* based on morphology, protease and gelatinase activity, and the cysteine proteinase gene

Gil M. Penuliar,[1*] Ronald R. Matias,[2] and Filipinas F. Natividad[2]
[1]Institute of Biology, University of the Philippines, Diliman, Quezon City 1101 Philippines;
[2]Research and Biotechnology Division, St. Luke's Medical Center, 279 E. Rodriguez Sr. Boulevard, Quezon City, 1102 Philippines
*Corresponding Author: Email: gmp@nih.go.jp; Fax: +81 3 5285 1173;Tel.: +81 3 5285 1111 ext. 2733

ABSTRACT

Acanthamoeba spp. are opportunistic pathogens that cause amebic keratitis and granulomatous amebic encephalitis in man. Recent attempts to correlate pathogenicity with species have been proven difficult due to inconsistencies in morphology-based classification. The objectives of this study were: (1) to compare clinical and environmental isolates based on morphology, protease and gelatinase activity, and the cysteine proteinase (CP) gene, and (2) to determine whether these features can be used to differentiate the isolates. Results show some degree of variation in trophozoite and cyst morphology. Zymography, demonstrated gross differences in banding patterns, and the protease activity of clinical isolates was greater than the environmental isolates (p-value < 0.01). Amplification of the CP gene yielded two bands in the environmental isolates, approximately 755 bp and 440 bp in length. In contrast, only one band, either the 755 bp or 440 bp band was amplified in the clinical isolates. The results confirmed the limitations of morphology in differentiating *Acanthamoeba* species, and suggest that zymography, protease activity, and detection of the CP gene are useful reference tests to distinguish pathogenic from non-pathogenic isolates.

Key words: *Acanthamoeba*, protease activity, cysteine proteinase gene

INTRODUCTION

Acanthamoeba is a free-living protozoan characterized by acanthapodia in the trophozoite stage and a double-walled cyst stage. It is widely distributed in nature due to its simple nutritional requirement and ability to encyst. Isolates have been obtained from soil and water samples, parts of plants and animals, contact lenses, and air-conditioning units (Zaragoza, 1994; Anderson, 1988). Based on clinical and epidemiological information, *Acanthamoeba* is considered to be an opportunistic pathogen of humans (Marciano-Cabral et al., 2000; Khan et al., 2001). Some species can cause fatal granulomatous amebic encephalitis (GAE), but most amebic infections are associated with eye keratitis (Armstrong 2000; Niederkorn et al., 1999). A number of researches have been conducted to identify *Acanthamoeba* isolates based on morphology, biochemical activity, and genetic composition. With the increasing number of medical cases associated with *Acanthamoeba*, some of these studies have attempted to correlate their results with virulence. Currently, pathogenicity in *Acanthamoeba* is demonstrated only when an isolate is obtained from a diseased tissue of a patient, or if an isolate can infect an animal model system (Vodkin et al., 1992). There is, therefore, a need to develop alternative methods that could effectively differentiate pathogenic from non-pathogenic isolates.

It has been reported that *Acanthamoeba*-conditioned medium (ACM) produces cytophatic effects in epithelial cells and corneal tissues, suggesting that secreted proteases are involved in epithelial-cell disaggregation (Khan et al., 2000; Badenoch et al., 1995). In 1993, Hadas and Mazur showed two major proteases in the ACM that could be separated electrophoretically. They reported a 35 kDa acidic protease and a 65 kDa alkaline protease that belonged to the cysteine type of proteases. Studies have shown that cysteine proteinases (CPs) are more active in pathogenic strains, and that pathogenicity is the result of proteolysis of the host's extracellular matrix by CPs (Yun et al., 1999; Tannich, 1998). Khan and Paget in 2002, on the other hand, used genus-specific primers for the PCR amplification of 18s rDNA to detect and speciate *Acanthamoeba* isolated from clinical and environmental sources. Their results suggested that significant variation exists between and within morphologically defined *Acanthamoeba* species.

The objectives of this study were: (1) to compare 2 clinical and 3 environmental isolates of *Acanthamoeba* based on morphology, protease and gelatinase activity, and the cysteine proteinase (CP) gene, and (2) to determine whether these characteristics can be used to effectively differentiate the isolates.

MATERIALS AND METHODS

Isolation, cloning, and culture of *Acanthamoeba* (De Jonckheere, 1980)

Soil samples collected from Davao (DAV), Iloilo (ILO), and Pangasinan (PAN), were suspended in sterile distilled water. Mixtures were allowed to stand for 15 min, and supernatants filtered with Whatman filter paper no. 4. Filter papers were inverted on 1.5% non-nutrient agar (NNA) plates, previously seeded with heat-killed *Escherichia coli*. Plates were incubated at 37°C and observed daily for trophozoites and cysts. After 1 week of incubation, sections on the plates containing large numbers of cysts were excised and transferred to new NNA plates. The two clinical isolates (RBD and NAG) used in the study were obtained from the Research and Biotechnology Division (RBD) of St. Luke's Medical Center, and the Institute of Tropical Medicine, in Nagasaki, Japan.

To axenize the environmental isolates, NNA plates were flooded with 10 ml sterile phosphate buffer saline (PBS), pH 7.2, and the cysts gently scraped off the plates with a sterile lancet. Suspensions were examined under a compound microscope, and diluted several times, until a single cyst of each isolate was obtained, and transferred to new NNA plates. Plates were incubated and observed daily for trophozoites and cysts. After one week, cysts were harvested as previously described, and suspensions centrifuged at 2,000 rpm for 10 min. Pellets were resuspended in 1N HCl for 3 h at room temperature (RT). HCl was removed after centrifugation at 2000 rpm for 10 min and pellets were washed 3 times with PBS. Cysts were resuspended in 25 ml proteose peptone yeast extract glucose solution (PPYG) and incubated at 37°C.

Trophozoite and cyst morphology

Acanthamoeba cultures were incubated for 10 min on ice and centrifuged at 700 rpm for 5 min. Supernatants were discarded and pellets resuspended in 1 ml PBS. Suspensions were examined under a 100X objective lens, oil immersion, and phase contrast microscope. One hundred trophozoites were measured and photographed with a Nikon™ digital camera. Cultures were allowed to encyst in NNA plates and the cysts harvested as previously described. The same number of cysts was measured and photographed.

Electron microscopy (Yagita et al., 1995)

Cysts were harvested and fixed with 2.5% buffered glutaraldehyde for 4 h. Samples were washed twice with 0.1M PBS for 10 min and centrifuged at 2,000 rpm for 5 min at RT. Cysts were fixed with 2% osmium tetroxide for 1 h and washed twice with 0.1M PBS. Pellets were transferred to 1.5 ml microcentrifuge tubes and dehydrated with 30% ethanol. Cysts were agitated for 10 min and centrifuged at 2,000 rpm for 2 min. The dehydration step was repeated using 70% ethanol, 95% ethanol, and 95% acetone. Samples were dehydrated 3 times with absolute acetone, placed in absolute propylene, and infiltrated with 1:1 propylene oxide and embedding media for 24 h. Cysts were transferred to bean capsules and infiltrated with 1:3 propylene oxide and embedding media for 24 h. Samples were centrifuged at maximum speed, and the supernatant replaced with absolute embedding media, and polymerized at 65°C for 24 h. Cysts were viewed and photographed under a JEOL JEM 1010™ transmission electron microscope.

Protease activity (Sarah et., 1994)

Three-day old cultures of *Acanthamoeba* were harvested as previously described, and counted. Approximately 2 x 10^6 cells were transferred to new culture flasks and incubated for 1 h at 37°C. Media were removed and replaced with 10 ml PBS. Cultures were incubated for 24 h at 37°C, and the trophozoites harvested by centrifugation at 700 rpm for 10 min at RT. ACM of the isolates were concentrated 8 to 10 folds by dialysis using polyethylene glycol. One hundred microliters of ACM was incubated with 200 µl 1 mg/ml azocasein for 1 h at RT. Reactions were stopped by adding 300 µl 10% trichloroacetic acid (TCA). Mixtures were shaken for 15 min and centrifuged at 3,000 rpm for 5 min. Five hundred microliters of 1M NaOH was added to 500 µl supernatant, and the absorbance read at 440 nm using a Spectra Max 190 ™ spectrophotometer. In another set-up, the ACM was pre-incubated with 1mM ethylenediamine tetra-acetic acid (EDTA) for 30 min before mixing with azocasein.

Gelatinase activity (Itoh et al., 1998)

Five microliters of concentrated ACM was mixed with 5 µl sample buffer, and electrophoresed in 10% SDS-PAGE with 0.1% gelatin. The gel was washed with 2.5% Triton X-100 for 2 h and incubated in 0.1 M glycine, pH 7.4, overnight at RT. The gel was stained with 0.5% [w/v] Coomassie Brilliant Blue R-250, overnight, and destained in acetic acid: methanol: water (10:30:60). Bands were visualized on a light box and photographed.

DNA extraction (Kilvington et al., 1991)

Trophozoites were harvested as previously described. Cell pellets were transferred to 1.5 ml microcentrifuge tubes and resuspended in 300 µl lysis buffer (100 mM disodium EDTA, 100 mM NaCI, 10 mM Tris hydrochloride [pH 8.0]), supplemented with 3 µl of RNAse (1mg/ml). Tubes were incubated for 30 min at 65°C, and centrifuged at 8,200 rpm for 10 min at 4°C. Supernatants were transferred to new tubes, mixed with 500 µl of phenol: chloroform: isoamyl alcohol (PCI), and centrifuged. Aqueous phases were transferred to new tubes and re-extracted with 500 µl PCI. After centrifugation, the aqueous phases were transferred to new tubes and mixed with 45 µl of 5 M ammonium acetate and 900 µl of cold absolute ethanol. Samples were incubated for 12 h at -20°C. Precipitated DNA was collected by centrifugation at 12,000 rpm for 15 min at 4°C. Pellets were washed with 70% ethanol, air dried for 30 min at RT, and resuspended in 30 µl sterile distilled water.

PCR amplification

A PCR mix for 5 samples was prepared composed of 108 µl sterile distilled water, 15 µl 10X PCR buffer, 4.8

µl 50 mM $MgCl_2$, 3 µl 20 mM dNTPs, 1.2 µl 250 U Taq polymerase, 3 µl 50 pM WRG3 forward primer, and 3 µl 50 pM WRG4 reverse primer. Twenty-three microliters of the PCR mix was loaded into five 0.5 ml PCR tubes and 10 ng of DNA sample was added. PCR tubes were loaded into an Eppendorf Mastercyler™ with the following conditions: initial denaturation for 10 min at 94°C, and subsequent denaturation for 1 min, annealing for 1.5 min at 52°C, extension for 1.5 min at 72°C, and denaturation for 1 min. Annealing and extension were repeated 38 times, followed by a final extension of 7 min at 72°C, and 10 min at 4°C. PCR products were electrophoresed in 2% agarose gel. Bands were visualized after ethidium bromide (1 µl/ml) staining.

Phylogenetic analysis (Felsenstein, 2000)

A similarity matrix was prepared from all the data obtained, and the characters were encoded as 1 and 0 to indicate the presence or absence of a character state, respectively; or to signify measurements above or below the mean of a set of values, respectively. The matrix was analyzed using PARS (Discrete character parsimony) in PHYLIP 3.6 and TREEVIEW 1.6.6.

STATISTICAL ANALYSIS

Data were analyzed using the single-factor ANOVA and correlation functions of Microsoft Excel statistical package (Microsoft corp. Redmond, WA, USA). Probability levels (*p*) less than 0.01 were considered significant.

RESULTS

Trophozoite and cyst morphology

The trophozoites of all the isolates were characterized by acanthapodia (Figure 1a). A clear separation of the hyaline ectoplasm and granular endoplasm was observed. The nucleus contained a centrally located nucleolus, and vacuoles were observed in the endoplasm. The diameter and nucleo-cytoplasmic (NC) ratio of the trophozoites varied (Table 1). RBD had the largest diameter (20.8 ± 0.7 µm), while ILO had the smallest (18.9 ± 0.5 µm). ILO, however, had the largest NC ratio (0.008), while NAG had the smallest (0.004).

The diameter and NC ratio of the cysts also varied (Table 1). RBD had the largest diameter (17.8 ± 3.1µm),

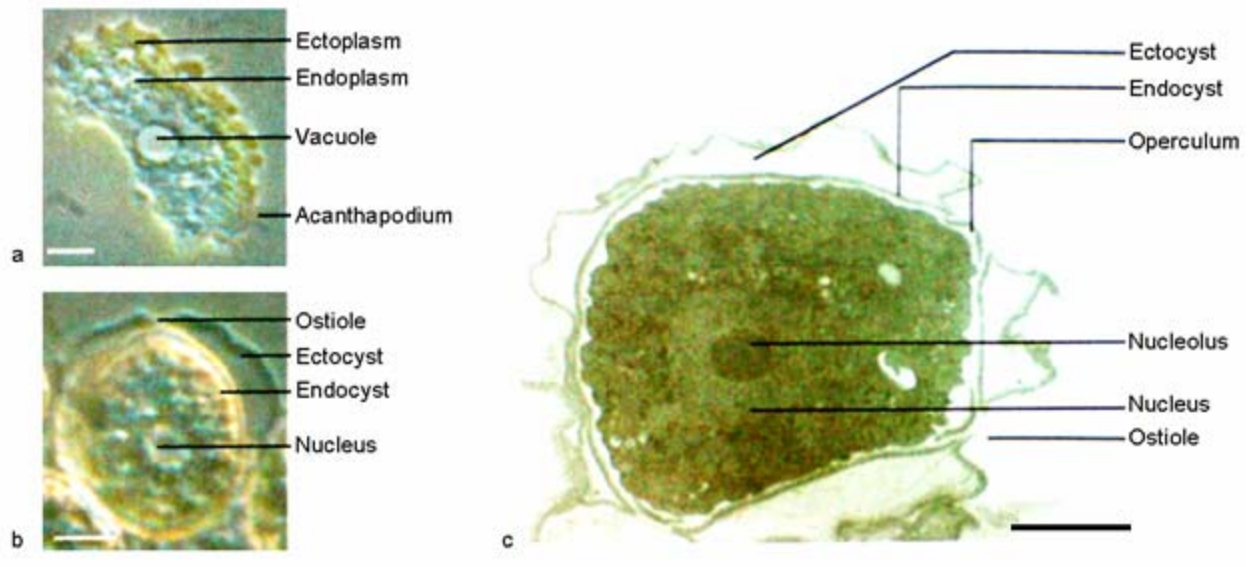

Figure 1: All of the isolates were identified as *Acanthamoeba* based on trophozoite and cyst morphology. (a) Trophozoites were characterized by the presence of acanthapodia projecting from the hyaline ectoplasm. (b) Cysts were bilaminar, composed of a wrinkled ectocyst and a smoother inner endocyst. The cyst walls meet at the region of the ostiole. (c) Electron photomicrograph of PAN showing the different parts of the cyst. The ostiole was covered from the inside by an operculum. The nucleus was large with a dense centrally located nucleolus. Bar = 5 µm.

Table 1. Morphology-based measurements. The diameter and nucleo-cytoplasmic (NC) ratio were determined for the trophozoites and cysts (n = 100), while the number of ostioles and ostiole diameter were determined from the cyst electron photomicrographs (n = 5).

	Trophozoite		Cyst		Cyst electron photomicrograph	
Isolate	Diameter (μm)	NC	Diameter (μm)	NC	No. of ostioles	Ostiole diameter (μm)
DAV	19.7 ± 0.5	0.006	16.4 ± 3.3	0.062	1 – 3	1.84 ± 0.44
ILO	18.9 ± 0.5	0.008	15.5 ± 3.6	0.061	1 – 2	1.61 ± 0.55
PAN	20.4 ± 0.6	0.006	17.0 ± 3.0	0.059	1 – 2	1.64 ± 0.40
NAG	20.5 ± 0.6	0.004	14.3 ± 2.9	0.069	1 – 2	1.75 ± 0.46
RBD	20.8 ± 0.7	0.006	17.8 ± 3.1	0.071	1 – 3	1.93 ± 0.42

while NAG had the smallest (14.3 ± 2.9 μm). RBD also had the largest NC ratio (0.071), while PAN had the smallest (0.059). The endocyst was predominantly spherical for all the isolates (Figure 1b), although a few cysts with polygonal and stellate-shaped endocysts were also observed (data not shown). The number of ostioles varied in number and diameter (Table 1). RBD and DAV had 1 to 3 ostioles, while NAG, ILO, and PAN had 1 to 2 ostioles. The ostioles of RBD had the largest diameter (1.93 ± 0.42 μm), while ILO had the smallest (1.61 ± 0.55 μm). Opercula were observed to cover the ostioles from the inside (Figure 1c). The cell membrane of the cysts was crenate in appearance and not closely apposed to the endocyst. A centrally located nucleolus was also observed (Figure 1c).

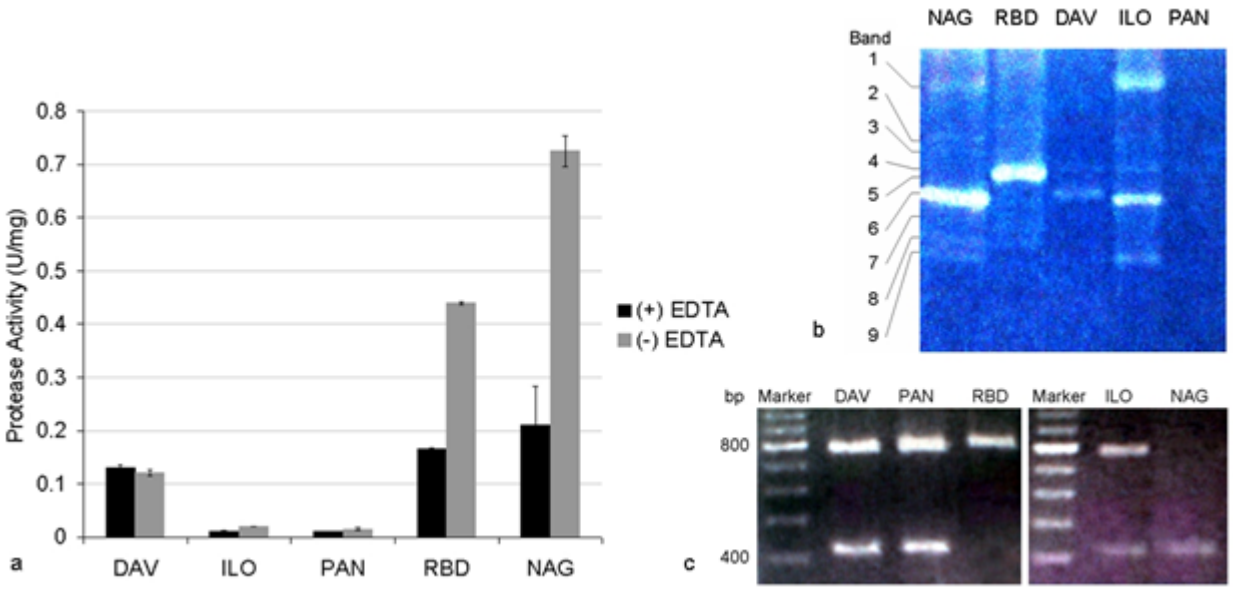

Figure 2. Protease and gelatinase activity, and CP gene amplification. (a) The protease activity of the clinical isolates was significantly higher than the environmental isolates (*p*-value < 0.01). A reduction in protease activity was observed when the samples were pre-incubated with 1mM EDTA. (b) The ACM of the isolates produced a total of 9 bands in 10% SDS-PAGE with 0.1% gelatin, indicating the presence of gelatinases. Bands 1, 2, 6, and 9 were observed in NAG and ILO. NAG lacked band 4 while DAV and PAN lacked band 8. Bands 3, 5, and 7 were observed only in NAG, DAV, and RBD, respectively. (c) Amplification of the CP gene yielded two bands in the environmental isolates, approximately 755 bp and 440 bp in length. In contrast, only the 755 bp band was amplified from RBD, while NAG produced only the 440 bp band.

Protease and gelatinase activity

The protease activity varied among the isolates (Figure 2a). NAG had the highest enzyme activity, while PAN had the lowest. The enyzme activity decreased when the ACM was pre-incubated with 1mM EDTA. The ACM of the isolates produced different banding patterns on the zymogram (Figure 2b). Nine different bands were observed. Bands 1, 2, 6, and 9 were observed in NAG and ILO. NAG lacked band 4, while DAV and PAN lacked band 8. Bands 3, 5, and 7 were observed only in NAG, DAV and RBD, respectively. ACM pre-incubated with 1mM EDTA produced the same number of bands in all the isolates (data not shown).

PCR amplification of the CP gene

Amplification of the CP gene yielded two bands in the environmental isolates, approximately 755 bp and 440 bp in length (Figure 2c). In contrast, only the 755 bp band was amplified from RBD, while NAG produced only the 440 bp band.

Phylogenetic analysis

Based from the first few trees generated, NAG separated early from the other isolates (data not shown). It was, therefore, omitted in the final analysis, to observe the relationship of RBD with the environmental isolates. ILO was observed to branch first, followed by RBD (Figure 3). PAN and DAV were the last to separate. When morphological characters alone were used, however, PAN and RBD separated from DAV and ILO (data not shown). This indicated that the range of values obtained from the morphological features were not able to distinguish the isolates.

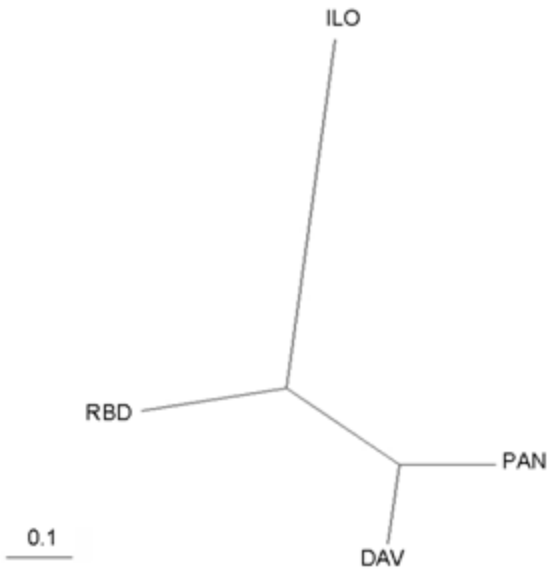

Figure 3. Phylogenetic analysis of RBD and the environmental isolates. NAG was not included in the final analysis because earlier analyses showed the early branching of NAG from the other isolates. The PARS utility in PHYLIP 3.6 and TREEVIEW 1.6.6 were used to generate the dendrogram. ILO was observed to branch first, followed by RBD. PAN and DAV were the last to separate. The early separation of ILO was consistent based on trophozoite diameter, while the branching of RBD correlated with the cyst diameter, protease activity, and CP gene amplification data.

DISCUSSION

Trophozoite and cyst morphology

The trophozoite morphology of the isolates corresponded to the descriptions made by Matias (1991) and Anderson (1988). The diameters varied significantly (p-value < 0.01), especially between ILO and the other isolates. A few trophozoites from each isolate were observed to have smaller and larger diameters than most of the trophozoites. Considering that the isolates were clonal, variations in diameter can be attributed to a transition from logarithmic growth to population growth deceleration. It was reported that marked changes in cell size and macromolecular composition are often observed during such transitions in *Acanthamoeba*. In addition, it was also reported that during each cell cycle, trophozoites release 12-37% of their weight (Anderson, 1988).

When the shape of the cell and form of the pseudopodia are similar, taxonomic distinctions in amoeba are then based on the nucleus and occurrence of cysts. NC ratio is the ratio of the volume of the nucleus and cytoplasm. Within isolates, the ratio is regulated by the activities of the nucleus, and variations in the ratio reflect differences in the age of the cell. It is reported to be high in dividing cells and low in old cells. Differences in the NC ratio of the trophozoites were significant (p-value < 0.01), but it did not differentiate the clinical from the environmental isolates.

The morphology of the cysts reflected the studies made by Yagita et al. (1995) and Lasman (1977). The size and shape of the cysts fell under Group III (Figure 1b,c). The group includes cysts with a mean diameter <18 μm, and an endocyst that is usually round (Visvesvara, 1991). The few polygonal and stellate-shaped cysts observed within isolates may be attributed to differences in the degree of desiccation, as this factor is reported to affect cyst morphology (Russel, 1996; Ma et al., 1990). Differences in cyst diameters were significant (p-value < 0.01), although it failed to distinguish the clinical from the environmental isolates. RBD, however, was observed to have a subpopulation of cysts with a diameter of 20 μm (data not shown). Variations in cyst diameter can also be due to the same factors affecting trophozoite diameter; but in conjunction with factors that lead to encystment in NNA plates like cell density and desiccation (Szenasi et al., 1998). It was, therefore, not surprising to observe some degree of correspondence (0.885) between the size of the cyst and trophozoite. Differences in the NC ratio of the cysts were significant (p-value < 0.01) and it divided the isolates into 2 groups. The NC ratio of the clinical isolates was at least seven units greater than the environmental isolates, indicating that the clinical isolates had larger nuclei.

The ectocyst was thicker than the endocyst for all isolates (Figure 1b,c). This was not surprising since the ectocysts is the part exposed to the environment. The ectocyst, however, appeared less compact than the endocyst. In 1998, Mehlotra tried to determine if pathogenic species of *Acanthamoeba* had thinner cyst wall than non-pathogenic species. The results of this study provided no clear answer (data not shown). The number of ostioles varied between isolates. Ostioles are passages through which the trophozoite leaves the cyst during excystment. It was, therefore, expected to observe some degree of correlation between the diameter of the ostiole with that of the trophozoites (0.6) and cysts (0.5). Each ostiole was covered from the inside by an operculum that had the same electron density as the endocyst. The ostiole is reported to function as an environmental sensor (Kilvington & White, 1994).

Protease and gelatinase activity

A number of researchers have demonstrated through cytotoxicity and colorimetric assays that *Acanthamoeba* secretes proteases (Khan et al., 2000; He et al., 1990). In this study, azocasein was used as a substrate to detect and quantify protease activity (Figure 2a). The results indicated that ACM contained proteases. In addition, the protease activity of the 5 isolates varied significantly (p-value < 0.01). Clinical isolates exhibited higher protease activity compared to environmental isolates. This result was consistent with previous findings that pathogenic species secrete more proteases than non-pathogenic species (Khan et al., 2000; Hadas & Mazur, 1993). Tannich (1998) suggested that the low amount of proteinases in non-pathogenic *Entamoeba* spp. was due to a lower number of proteinase expressing genes. The present data suggest that differences in protease activity can be used as a marker for differentiating clinical and environmental isolates of *Acanthamoeba*.

Results also showed that EDTA significantly inhibited ACM protease activity (p-value < 0.01). EDTA is a general protease inhibitor that chelates bivalent metal ions in enyzmes. The finding, however, did not correlate with the work of Mitro et al. (1994), who reported that no significant inhibition of protease activity was observed with 10 mM EDTA. In addition, Hadas and Mazur (1993), reported that 10 mM EDTA enhanced protease activity. The concentration used in their studies, however, was different from the concentration used in this study. EDTA works effectively at a concentration of 1 mM to 10 mM, and can be inhibitory or stimulatory depending on its concentration. Alfieri et al. (2000) reported that the hydrolysis of azocasein was predominantly associated with the activity of cysteine proteinases. However, since the inhibitor used was not specific for cysteine proteinases, the observed ACM protease activity may be due to other proteases.

To visualize the protease activity, ACM was electrophoresed in an SDS-PAGE with 0.1% gelatin (Figure 2b). The bands observe indicated the presence of gelatinases. Moreover, variations in banding pattern intensity, suggested that various gelatinases were

secreted in different amounts by the isolates. The finding correlated with the work of Mitro et al. (1994), that *Acanthamoeba* secretes different types of proteases. Although the banding patterns did not differentiate the clinical and environmental isolates, the variations observed can still be used to characterize the isolates individually. Pre-incubation of the ACM with 1 mM EDTA produced the same number of bands, suggesting that gelatinases were not inhibited by EDTA.

Detection of the CP gene

With the developments of new tools in molecular biology, several workers have attempted to identify markers at the nucleic acid level to distinguish pathogenic from non-pathogenic isolates (Mirelman et al., 1996). In this study, primers WRG3 and WRG4 were used to detect the CP gene in the genomic DNA of *Acanthamoeba*. The primers were designed to amplify a 755 bp fragment of the CP (*ehcp1*) gene found in *Entamoeba histolytica*. The primers were able to amplify certain regions in the DNA of *Acanthamoeba*, indicating the presence of conserved regions between *E. histolytica* and *Acanthamoeba* (Figure 2c).

Variations in the PCR products indicated that the clinical isolates differ not only from the environmental isolates but also from each other. Furthermore, amplification of the 440 bp band in NAG and environmental isolates, suggested the presence of incomplete repeats of the target sequence in the isolates. The amplification was specific, since the band consistently appeared in all the trials. The detection of the CP gene with primers designed for *E. histolytica*, was not surprising since it had been reported that closely related species contain the same gene for CP. The gene, however, may vary due to numerous nucleotide exchanges, insertions, and deletions (Willhoeft et al., 1999; Mirelman et al., 1996).

Phylogenetic analysis

The PARS utility in PHYLIP 3.6 was used because the program allows users to analyze similarity matrices based on the assumptions that ancestral states are unknown and that characters evolve independently (Felsenstein, 2000). NAG was not included in the final analysis because earlier analyses showed the early branching of NAG from the other isolates (data not shown). Considering the geographical location where NAG was isolated, and based on the PCR data, it was not surprising that NAG was not as closely related to the environmental isolates compared to RBD. The early separation of ILO was consistent based on trophozoite diameter, while the branching of RBD correlated with the cyst diameter, protease activity, and CP gene amplification data.

In conclusion, the results obtained from this study verified the limitations inherent in morphology-based methods of identification. While trophozoite and cyst morphology effectively differentiate *Acanthamoeba* from other protozoa, morphological characters cannot distinguish the isolates based on pathogenicity. A practical approach to solve this problem is to include more stable characters like enzyme activity and amplification of conserved genes, which has been shown in this study, and by previous researchers, to be valuable tools in differentiating pathogenic from non-pathogenic isolates.

ACKNOWLEDGMENTS

The authors thank Dr. Gloria L. Enriquez, Dr. Windell L. Rivera, and the Research and Biotechnology Division (RBD) of St. Luke's Medical Center.

REFERENCES

Alfieri, S., C. Correla, S. Motegi, & E. Pral, 2000. Proteinase activities in total extracts and in medium conditioned by *Acanthamoeba polyphaga* trophozoites. *J. Parasitol.* 86(2): 220-227.

Anderson, R., 1988. Comparative Protozoology: Ecology, Physiology, Life History. New York: Springer-Verlag.

Armstrong, M., 2000. The pathogenesis of human *Acanthamoeba* infections. *Infect Dis. Rev.* 2(2): 65-73.

Badenoch, P., M. Adams, & D. Coster, 1995. Corneal virulence, cytophatic effect on human keratocytes and genetic characterization of *Acanthamoeba*. *Int. J. Parasitol.* 25(2): 229-239.

De Jonckheere, J., 1980. Growth characteristics, cytopathic effect in cell culture, and virulence in mice of 36 type strains belonging to 19 different *Acanthamoeba* spp. *Appl Environ Microbiol.* 39(4): 681-5.

Felsenstein, J., 2000. PHYLIP 3.6: Phylogeny Inference Package. Available from URL: http://evolution.genetics.washington.edu/phylip/

Hadas, E. & T. Mazur, 1993. Biochemical markers of pathogenicity and virulence of *Acanthamoeba* sp. strains. *Parasitol. Res.* 79(8): 696-698.

He, Y., J. Niederkorn, J. McCulley, G. Stewart, D. Meyer, R. Silvany, & J. Doughtery, 1990. *In vivo* and *in vitro* collagenolytic activity of *Acanthamoeba castellani*. *Invest. Opthal. Vis. Sci.* 31:2235-2240.

Itoh, Y., A. Ito, K. Iwata, K. Tanzawa, Y. Mori, & H. Nagase, 1998. Plasma membrane-bound tissue inhibitor of metallopeptidases (TIMP)-2 specifically inhibits matrix metallopeptidase 2 (gelatinase A) activated on the cell surface. *J. Biol. Chem.* 273: 24360-24367.

Khan, N. & T. Paget, 2002. Molecular tools for speciation and epidemiological studies of *Acanthamoeba*. *Curr. Microbiol.* 44(6): 444-4449.

Khan, N., E. Jarroll, & T. Paget, 2001. *Acanthamoeba* can be differentiated clinically by the polymerase chain reaction and simple plating assays. *Curr. Microbiol.* 43: 204-208.

Khan, N., E. Jaroll, N. Panjawani, Z. Cao, & T. Paget, 2000. Proteases as marker for differentiation of pathogenic and non-pathogenic species of *Acanthamoeba*. *Journal of Clinical Microbiology.* 38(8): 2858-2861.

Kilvington, S. & P. White, 1994. *Acanthamoeba*: biology, ecology, and human disease. *Review in Medical Microbiology.* 5(1): 12-20.

Kilvington, S., J. Beeching, & D. White, 1991. Differentiation of *Acanthamoeba* strains from infected corneas and the environment by using restriction endonuclease digestion of whole-cell DNA. *J. Clin. Microbiol.* 29(2): 310-4.

Lasman, M., 1977. Light and electron microscopic observations on encystment of *Acanthamoeba palestinensis* Reich. *J. Protozool.* 24(2): 244-248.

Ma, P., G. Visvesvara, A. Martinez, F. Theodore, D. Pierre-Mare, & T. Sawyer, 1990. *Naegleria* and *Acanthamoeba* infections. *Rev. Infect. Dis.* 12: 490-573.

Marciano-Cabral, F., R. Puffenbarger, & G. Cabral, 2000: The increasing importance of *Acanthamoeba* infections. *J. Eukaryot. Microbiol.* 47: 29-36.

Matias, R., J. Schotteliu, C. Raddatz, & R. Michel, 1991. Species identification and characterization of a *Acanthamoeba* strain from human cornea. *Parasitology Research.* 77(6): 469-474.

Mehlotra, R., 1998. Differentiation of pathogenic and non-pathogenic *Entamoeba*: has the question been answered? *Indian Society of Gastroenterology.* 17: 58-60.

Mirelman, D., Y. Michamowitzi, B. Bohn-Gloning, & B. Walderich, 1996. A homologue of the cysteine proteinase gene (ACP1) of pathogenic *Entamoeba histolytica* in present in non-pathogenic *E. dispar* strains. *Parasitol. Res.* 36: 518-543.

Mitro, K., A. Bhagavathiammi, G. Bobbett, J. Mckerrow, B. Chokshi, & R. James, 1994. Partial characterization of the proteolytic secretions of *Acanthamoeba polyphaga. Expt. Parasitol.* 78(4): 377-378.

Niederkorn, J., Y. Alizadeh, H. Lether, & J. McCulley, 1999. The pathogenesis of *Acanthamoeba* keratitis. *Microbes Infect.* 1(6): 437-443.

Russel, A., 1996. The lethal effects of biguanides on cysts and trophozoites of *Acanthamoeba castellani*. *J. Appl. Bacteriol.* 8(1): 73-77.

Sarah, G., S. de la Motte, & W. Wagner, 1994. Protease methods, p. 28. In RJ Beynon and JS Bond (ed), proteolytic enzymes, a practical approach, 2nd ed. IRL, Oxford, UK.

Szensi, S., T. Endo, K. Yagita, & E. Nagy, 1998. Isolation, identification, and increasing importance of free-living amoeba causing human diseases. *J. Med. Microbiol.* 47: 5-16.

Tannich, E., 1998. *Entamoeba histolytica* and *E. dispar*: comparison of molecules considered important for host tissue destruction. Transactions of the royal society of tropical medicine and hygiene. 92: 593-596.

Visvesvara, G., 1991. Classification of *Acanthamoeba*. *Rev Infect Dis.* 13 Suppl 5:S369-72.

Vodkin, M., D. Howe, G. Visvesvara, & G. McLaughlin, 1992. Identification of *Acanthamoeba* at the Genetic and Specific Levels Using the Polymerase Chain Reaction. *J. Protozool.* 39(3): 378-385.

Willhoeft, U., L. Hamann, & E. Tannich, 1999. A DNA corresponding to the gene encoding cysteine proteinase 5 in *Entamoeba histolytica* in present and positionally conserved but highly degenerated in E. dispar. *Infection and Immunity.* 67(11): 5925-5929.

Yagita, K., R. Matias, T. Yasuda, F. Natividad, G. Enriquez, & T. Endo, 1995. *Acanthamoeba* sp. from the Philippines: electron microscopy studies on naturally occurring bacterial symbionts. *Parasitology Research.* 81: 98-102.

Yun, H., K. Kim, S. Park, U. Hwang, K. Hong, J. Ryu, & D. Min. 1999. Cloning of a cysteine proteinase gene from *Acanthamoeba culbertsonii*. *Mol. Cells.* 9(5): 491-496.

Zaragosa, S., 1994. Ecology of free-living amoeba. *Crit. Rev Microbiol.* 20(3): 225-241.